Emerging Materials Research
Volume 2 Issue EMR1

Symmetry-mode-based atomic scale formalism of lattice dynamics
Seman, Moon and Ahn

ice | science

Pages 5–16 http://dx.doi.org/10.1680/emr.12.00023
Research Article
Received 18/07/2012 Accepted 03/12/2012
Published online 08/12/2012
Keywords: condensed matter/materials science/lattice dynamics/structural properties

ice Institution of Civil Engineers publishing

Symmetry-mode-based atomic scale formalism of lattice dynamics

Tsezar F. Seman
Department of Physics, New Jersey Institute of Technology, Newark, NJ, USA

Keun Hyuk Ahn PhD*
Department of Physics, New Jersey Institute of Technology, Newark, NJ, USA

Jichan Moon
Department of Physics, Konkuk University, Seoul, South Korea

The authors present classical and quantum mechanical descriptions of lattice dynamics, from the atomic to the continuum scale, using atomic scale symmetry modes and their constraint equations. This approach is demonstrated for a one-dimensional chain and a two-dimensional square lattice with a monatomic basis. For the classical description, the authors find that rigid modes, in addition to the distortional modes found before, are necessary to describe the kinetic energy. The long-wavelength limit of the kinetic energy terms expressed in terms of atomic scale modes is shown to be consistent with the continuum theory, and the leading order corrections are obtained. For the quantum mechanical description, the authors find conjugate momenta for the atomic scale symmetry modes. In direct space, graphical rules for their commutation relations are obtained. Commutation relations in the reciprocal space are also calculated. As an example, phonon modes are analyzed in terms of symmetry modes. The authors briefly discuss how the approach presented here, based on atomic scale symmetry modes, could be useful for the study of atomic scale dynamics in solid–solid phase transitions in complex emergent materials, in which competition between structural phases and nonlinearity of the lattice energy plays an important role.

List of notations

A_1, A_2, A_3 = Moduli for modes $e_1(\vec{i})$, $e_2(\vec{i})$, and $e_3(\vec{i})$ in V_{sq}

$A_3^{'}$ = Negative of moduli for $e_3(\vec{i})$ in V_{rec}

$a = (A_1 - A_2 + A_3)/(A_1 + A_2 - A_3)$

B = Modulus for modes $s_x(\vec{i})$ and $s_y(\vec{i})$ in V_{sq}

C_3 = Coupling coefficient between $s_x(\vec{i})^2 - s_y(\vec{i})^2$ and $e_3(\vec{i})$ in V_{multi}

$C_x, C_y = \cos k_x, \cos k_y$

$e(\vec{i}), e_1(\vec{i}), e_2(\vec{i}), e_3(\vec{i})$ = Distortive symmetry mode for 1D chain, and dilatational, shear and deviatoric symmetry modes for 2D square lattice

$f(k), f_n(\vec{k})$ = Constraint equations for chain and square lattice $(n = 1 \ldots 6)$

F_3 = Coefficient for the fourth order term in V_{rec}

G_1, G_2, H_1, H_2 = Coefficients for the fourth and sixth order term in V_{multi}

$i, \vec{i}$ = Indices for sites for chain and square lattice

K = spring constant for chain

$k, \vec{k}$ = Dimensionless reciprocal space variables for chain and square lattice

$L_{\text{chain}}, \tilde{L}_{\text{chain}}, \tilde{L}_{\text{sq}}$ = Lagrangian for chain and modified Lagrangians for chain and square lattice

$L_{\text{rec}}, L_{\text{multi}}$ = Lagrangians for rectangular lattice and lattice with multiple local and global energy minima

M = Mass of atom

$P_m(i), P_m(\vec{i})$ = Conjugate momenta of symmetry modes m for chain and square lattice

***Corresponding author e-mail address:** kenahn@njit.edu

p_i, p_i^x, p_i^y = Momenta of atoms for chain and square lattice

$r(\vec{i})$ = Rotational symmetry mode for square lattice

S_x, S_y = $\sin k_x$, $\sin k_y$

$s_x(\vec{i}), s_y(\vec{i}), s_+(\vec{i}), s_-(\vec{i})$ = Staggered symmetry modes for square lattice

T_{sq} = Kinetic energy for square lattice

t(i) = Translational symmetry mode for chain

$t_x(\vec{i}), t_y(\vec{i}), t_+(\vec{i}), t_-(\vec{i})$ = Translational symmetry modes for square lattice

u_i, u_i^x, u_i^y = Displacements of atoms for chain and square lattice

V, V_{sq}, V_{rec}, V_{multi} = Potential energy for square lattice, rectangular lattice, and lattice with multiple local and global energy minima

$\beta_1, \beta_2, \beta_3, \beta_4, \beta_5$ = $1-\cos k_x \cos k_y, -\sin k_x \sin k_y, \cos k_x - \cos k_y, (1-\cos k_x)(1-\cos k_y), (1+\cos k_x)(1+\cos k_y)$

$\gamma_{ss'}(\vec{k}), \gamma_{ss'}^{(0)}(\vec{k}), \gamma_{ss'}^{(1)}(\vec{k})$ = Kinetic energy coefficients and their first and second order terms in long wavelength limit for square lattice (s, s' = 1, 3)

$\lambda(k), \lambda_n(\vec{k})$ = Lagrangian multipliers for chain and square lattice (n = 1 ... 6)

ω = Angular frequency of normal mode

1. Introduction

The dynamics at nanometer length scale has been a focus of recent attention in materials research.[1] In particular, emerging materials with competing ground states, such as high-temperature superconducting cuprates, colossal magnetoresistive manganites[2,3,4] and multiferroic materials often show dynamic nanometer scale features, for example, stripes in cuprates[5,6] and anisotropic correlations in manganites.[7,8] Furthermore, recent advances in time-resolved X-ray technique have allowed experimenters to directly probe lattice dynamics in atomic scale.[9] It is believed that understanding these nanoscale features and their dynamics is essential to explain macroscopic properties of these materials.

For the description of mesoscopic scale domain structures and their dynamics, phenomenological Ginzburg-Landau formalism has been very successful.[10,11] One of the keys for such a success is the use of symmetry in the definition of variables, which makes the selection of free energy terms self-evident. Motivated by the success of the Ginzburg-Landau approach for the continuum, symmetry-based atomic scale description of lattice distortions has been recently proposed and demonstrated for a two-dimensional square lattice.[12] In this approach, atomic scale symmetry modes are defined on a plaquette of atoms and are used to express potential energy terms associated with lattice distortions. This method has been used to understand atomic scale structure of twin boundaries,[12] antiphase boundaries and their electronic textures,[13] strain-induced metal–insulator phase coexistence in manganites,[8] superconducting-order parameter textures around structural defects[14] and the coupling between electronic nematic order parameter and structural domains in metamagnets near a quantum critical point.[15] Thus far, this approach has been used for static lattices, or the relaxation of lattice distortions introduced through the Euler method,[10] which does not require kinetic energy terms. In the current article, the authors present the study on how the approach based on atomic scale symmetry modes can be extended to describe lattice dynamics, within the scope of both classical and quantum mechanical formalism. In section 2, the authors discuss how to express kinetic energy term in symmetry modes, present the study within the formalism of classical mechanics and compare the result with the continuum results.[11] The authors formulate quantum mechanics in terms of atomic scale symmetry modes in section 3. The authors present a demonstration of symmetry-mode-based approach for lattice dynamics, that is, the phonon-mode analysis in terms of symmetry modes in section 4. Brief discussion on how to apply the method for the simulation of atomic scale dynamics in solid–solid phase transitions is given in section 5. The conclusion is given in section 6.

2. Classical formalism

2.1 One-dimensional lattice with a monatomic basis

Using a one-dimensional lattice with a monatomic basis shown in Figure 1, the authors demonstrate the concept of the mode-based description of lattice dynamics. The displacements of atoms are represented by u_i, where i being an index for the site. To be specific, the authors assume that the interaction between the nearest neighbor atoms are described by a spring with a spring constant K, while other potential energy terms are negligible, as represented by the following Lagrangian,

$$L_{\text{chain}} = \sum_i \frac{1}{2} M \dot{u}_i^2 - \frac{1}{2} K (u_{i+1} - u_i)^2 \quad (1)$$

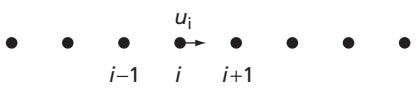

Figure 1. One-dimensional lattice with a monatomic basis.

where, M is the mass of the atom. The authors take a two-atom unit as a motif for this lattice and define the symmetry modes, $e(i)$ and $t(i)$,

2. $$e(i) \equiv \frac{1}{\sqrt{2}}(u_{i+1} - u_i)$$

3. $$t(i) \equiv \frac{1}{\sqrt{2}}(u_{i+1} + u_i)$$

where a normalization factor is chosen according to the number of displacement variables in the definition. These modes are also shown in Figure 2.

The two variables, e and t, correspond to the distortion and rigid translation of the motif, respectively. Since the two modes are defined from one physically independent displacement variable at each site i, these modes are related through one constraint equation shown below in the reciprocal space and direct space, respectively.

4. $$f(k) \equiv (e^{ik} + 1)e(k) - (e^{ik} - 1)t(k) = 0$$

5. $$e(i+1) + e(i) - t(i+1) + t(i) = 0$$

In terms of these modes, the Lagrangian in Equation (1) is expressed in the following way

6. $$L_{\text{chain}} = \sum_i \frac{1}{2}\left(\frac{M}{2}\right)[\dot{e}(i)^2 + \dot{t}(i)^2] - \frac{1}{2}(2K)e(i)^2$$

The result shows that introduction of atomic scale rigid modes, such as t, which are not considered in the previous work,[12] allows kinetic energy term being expressed in a quadratic form. To obtain equations of motion, the authors modify L_{chain} with a Lagrange multiplier $\lambda(k)$, as shown below.

7. $$\tilde{L}_{\text{chain}} = \sum_k \frac{1}{2}\left(\frac{M}{2}\right)[\dot{e}(k)\dot{e}(-k) + \dot{t}(k)\dot{t}(-k)] - \frac{1}{2}(2K)e(k)e(-k) + \lambda(k)f(-k)$$

The Lagrangian formalism of dynamics leads to the two equations of motion,

Figure 2. Symmetry modes for the one-dimensional chain in Figure 1.

8. $$\frac{M}{2}\ddot{e}(k) + 2Ke(k) - \lambda(k)(e^{-ik} + 1) = 0$$

9. $$\frac{M}{2}\ddot{t}(k) + \lambda(k)(e^{-ik} - 1) = 0$$

and a well-known dispersion relation for the one-dimensional chain,[16]

10. $$\omega = \sqrt{\frac{K}{M}(1 - \cos k)}$$

This result shows that the lattice dynamics can be studied within the framework of atomic scale symmetry modes and their constraint equations, without using the displacement variables explicitly.

Anharmonicity of one-dimensional chains is important to understand nonlinear excitations, such as solitons, kink-solitons, intrinsically localized modes and breathers.[17,18] Atomic scale modes, e and t, found here can be used to incorporate such anharmonicity into the Hamiltonian, which, along with their constraint equations, would provide a formalism to study the dynamics of nonlinear excitations in one-dimensional chains. In the next subsection, the authors demonstrate how the mode-based approach is applied to lattice dynamics for a two-dimensional square lattice with a monatomic basis.

2.2 Two-dimensional square lattice with a monatomic basis

Symmetry-based atomic scale description of lattice distortions for a two-dimensional square lattice with a monatomic basis, shown in Figure 3, has been studied previously,[12] where three long-wavelength modes, dilatational e_1, shear e_2 and deviatoric e_3 modes and two short-wavelength modes, s_x and s_y, are defined, as shown in Figure 4. In terms of displacement variables u_i^x and u_i^y, and i_x

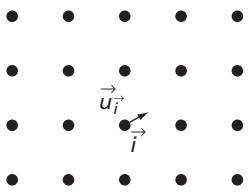

Figure 3. Two-dimensional square lattice with a monatomic basis.

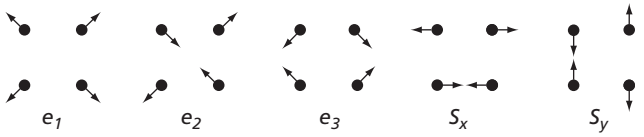

Figure 4. Distortional symmetry modes of the motif for the two-dimensional square lattice with a monatomic basis in Figure 3.

and i_y representing site indices, these distortional symmetry modes are expressed as follows:

11. $$e_1(\vec{i}) = \frac{1}{2\sqrt{2}} \left(-u_{\vec{i}}^x - u_{\vec{i}}^y + u_{\vec{i}+10}^x - u_{\vec{i}+10}^y - u_{\vec{i}+01}^x + u_{\vec{i}+01}^y + u_{\vec{i}+11}^x + u_{\vec{i}+11}^y\right)$$

12. $$e_2(\vec{i}) = \frac{1}{2\sqrt{2}} \left(-u_{\vec{i}}^x - u_{\vec{i}}^y - u_{\vec{i}+10}^x + u_{\vec{i}+10}^y + u_{\vec{i}+01}^x - u_{\vec{i}+01}^y + u_{\vec{i}+11}^x + u_{\vec{i}+11}^y\right)$$

13. $$e_3(\vec{i}) = \frac{1}{2\sqrt{2}} \left(-u_{\vec{i}}^x + u_{\vec{i}}^y + u_{\vec{i}+10}^x + u_{\vec{i}+10}^y - u_{\vec{i}+01}^x - u_{\vec{i}+01}^y + u_{\vec{i}+11}^x - u_{\vec{i}+11}^y\right)$$

14. $$s_x(\vec{i}) = \frac{1}{2}\left(u_{\vec{i}}^x - u_{\vec{i}+10}^x - u_{\vec{i}+01}^x + u_{\vec{i}+11}^x\right)$$

15. $$s_y(\vec{i}) = \frac{1}{2}\left(u_{\vec{i}}^y - u_{\vec{i}+10}^y - u_{\vec{i}+01}^y + u_{\vec{i}+11}^y\right)$$

where 10, 01 and 11 represent the offset of the site index by (1,0), (0,1) and (1,1), respectively.

Instead of s_x and s_y modes, the following s_+ and s_- modes can be also used.

16. $$s_+(\vec{i}) = \frac{1}{\sqrt{2}}[s_x(\vec{i}) + s_y(\vec{i})]$$

17. $$s_-(\vec{i}) = \frac{1}{\sqrt{2}}[s_x(\vec{i}) - s_y(\vec{i})]$$

These five modes have been used to express various harmonic and anharmonic potential energy terms[8,12,13] but are not sufficient to represent kinetic energy terms in a simple quadratic form.

In current work, the authors show that additional modes associated with the rigid motion of the motif, similar to the mode t in the one-dimensional chain, allow formalism entirely based on symmetry modes without resorting to displacement variables. Three rigid modes for the two-dimensional square lattice are shown in Figure 5 and are defined as follows:

18. $$t_x(\vec{i}) = \frac{1}{2}\left(u_{\vec{i}}^x + u_{\vec{i}+10}^x + u_{\vec{i}+01}^x + u_{\vec{i}+11}^x\right)$$

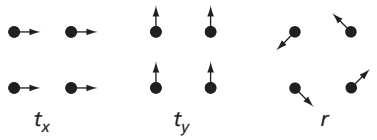

Figure 5. Rigid symmetry modes of the motif for the two-dimensional square lattice with a monatomic basis in Figure 3.

19. $$t_y(\vec{i}) = \frac{1}{2}\left(u_{\vec{i}}^y + u_{\vec{i}+10}^y + u_{\vec{i}+01}^y + u_{\vec{i}+11}^y\right)$$

20. $$r(\vec{i}) = \frac{1}{2\sqrt{2}} \left(u_{\vec{i}}^x - u_{\vec{i}}^y + u_{\vec{i}+10}^x + u_{\vec{i}+10}^y - u_{\vec{i}+01}^x - u_{\vec{i}+01}^y - u_{\vec{i}+11}^x + u_{\vec{i}+11}^y\right)$$

The first two modes, t_x and t_y, correspond to rigid translations of the motif along x and y direction, and the mode r represents a rigid rotation of the motif. Following t_+ and t_- modes can be also used as alternatives to t_x and t_y.

21. $$t_+(\vec{i}) = \frac{1}{\sqrt{2}}[t_x(\vec{i}) + t_y(\vec{i})],$$

22. $$t_-(\vec{i}) = \frac{1}{\sqrt{2}}[t_x(\vec{i}) - t_y(\vec{i})]$$

Straight-forward expansion shows that the kinetic energy of the lattice is expressed in terms of the eight symmetry modes in the following quadratic form, with M being the mass of the atom.

23. $$T_{\text{sq}} = \sum_{\vec{i}} \frac{1}{2} M[(\dot{u}_{\vec{i}}^x)^2 + (\dot{u}_{\vec{i}}^y)^2]$$

24. $$T_{\text{sq}} = \sum_{\vec{i}} \frac{1}{2}\left(\frac{M}{4}\right) [\dot{e}_1(\vec{i})^2 + \dot{e}_2(\vec{i})^2 + \dot{e}_3(\vec{i})^2 + \dot{s}_x(\vec{i})^2 + \dot{s}_y(\vec{i})^2 + \dot{t}_x(\vec{i})^2 + \dot{t}_y(\vec{i})^2 + \dot{r}(\vec{i})^2]$$

As discussed in previous work,[12] constraint equations are found from the relations between symmetry modes and displacement variables in the reciprocal space. The authors first represent $(u_{\vec{k}}^x, u_{\vec{k}}^y)$ in terms of $(s_x(\vec{k}), s_y(\vec{k}))$ by inverting the linear relations between them and replace in the expressions with other modes, which lead to six constraint equations.

25. $$\sin\frac{k_x}{2}\cos\frac{k_y}{2}s_x(\vec{k})+\cos\frac{k_x}{2}\sin\frac{k_y}{2}s_y(\vec{k}) -\sqrt{2}i\sin\frac{k_x}{2}\sin\frac{k_y}{2}e_1(\vec{k})=0$$

26. $$\cos\frac{k_x}{2}\sin\frac{k_y}{2}s_x(\vec{k})+\sin\frac{k_x}{2}\cos\frac{k_y}{2}s_y(\vec{k}) -\sqrt{2}i\sin\frac{k_x}{2}\sin\frac{k_y}{2}e_2(\vec{k})=0$$

27. $$\sin\frac{k_x}{2}\cos\frac{k_y}{2}s_x(\vec{k})-\cos\frac{k_x}{2}\sin\frac{k_y}{2}s_y(\vec{k}) -\sqrt{2}i\sin\frac{k_x}{2}\sin\frac{k_y}{2}e_3(\vec{k})=0$$

28. $$\cos\frac{k_x}{2}\sin\frac{k_y}{2}s_x(\vec{k})-\sin\frac{k_x}{2}\cos\frac{k_y}{2}s_y(\vec{k}) +\sqrt{2}i\sin\frac{k_x}{2}\sin\frac{k_y}{2}r(\vec{k})=\mathbf{0}$$

29. $$\cos\frac{k_x}{2}\cos\frac{k_y}{2}s_x(\vec{k})+\sin\frac{k_x}{2}\sin\frac{k_y}{2}t_x(\vec{k})=0,$$

30. $$\cos\frac{k_x}{2}\cos\frac{k_y}{2}s_y(\vec{k})+\sin\frac{k_x}{2}\sin\frac{k_y}{2}t_y(\vec{k})=0.$$

The eight symmetry modes shown in Figures 4 and 5 can be obtained by applying group theory to four atoms in square geometry in two-dimensional space, as done in quantum molecular chemistry.[19] The same approach used for molecules can be applied to the motifs of the infinite lattices even though the neighboring motifs share atoms. The kinetic energy shown above does not include any double counting of the kinetic energies, in spite of the overlapping definition of the motifs. An important difference between the results for molecule and lattice is the presence of the constraint equations, equations 25–30, because, unlike in molecule, each atom is shared by multiple motifs in the lattice. These constraints generate an effective long range anisotropic interaction between distortions of motifs separated from each other, which has a far reaching consequence, for example, in solid–solid-phase transitions.[8,10,11,12]

With the constrain equations, the modified Lagrangian for the square lattice is now

31. $$\tilde{L}_{\mathrm{sq}}=T_{\mathrm{sq}}-V+\sum_{n=1}^{6}\sum_{\vec{k}}\lambda_n(\vec{k})f_n(-\vec{k}),$$

where V is the potential energy, $\lambda_n(\vec{k})$ are Lagrange multipliers and $f_n(\vec{k})=0$ are the six constraint equations 25–30. By solving the Lagrangian equations, the authors find dynamic properties of the lattice in terms of the symmetry modes. As with the Ginzburg-Landau approach being useful for the description of mesoscale dynamics, the authors expect that this approach based on atomic scale symmetry modes would be useful for the description of atomic scale dynamics, particularly, when anharmonicity plays an essential role.

2.3 Comparison with continuum description of lattice dynamics

The authors compare the atomic scale theory developed in the previous subsection with an existing continuum theory of lattice dynamics. Either by using the definitions, equations 11 and 13, or by using the constraint equations, the authors express the kinetic energy for the square lattice, equations 23 and 24, in terms of e_1 and e_3,

32. $$T_{\mathrm{sq}}=\sum_{\vec{k}}\sum_{s=1,3}\sum_{s'=1,3}\frac{1}{2}M\gamma_{ss'}(\vec{k})\dot{e}_s(\vec{k})\dot{e}_{s'}(-\vec{k}),$$

where

33. $$\gamma_{11}(\vec{k})=\gamma_{33}(\vec{k})=\frac{1-\cos k_x\cos k_y}{\sin^2 k_x\sin^2 k_y},$$

34. $$\gamma_{13}(\vec{k})=\gamma_{31}(\vec{k})=\frac{\cos k_x-\cos k_y}{\sin^2 k_x\sin^2 k_y}.$$

To compare with a continuum theory, the authors take the long-wavelength limit and obtain the following leading order term for $\gamma_{ss'}$,

35. $$\gamma_{ss'}^{(0)}(\vec{k})=\begin{pmatrix}\frac{k_x^2+k_y^2}{2k_x^2k_y^2} & \frac{k_y^2-k_x^2}{2k_x^2k_y^2}\\ \frac{k_y^2-k_x^2}{2k_x^2k_y^2} & \frac{k_x^2+k_y^2}{2k_x^2k_y^2}\end{pmatrix}$$

This term is identical to equation (3.12a) in a previous work[11] (e_3 here corresponds to e_2 in Lookman *et al.*, 2003), where Lookman *et al.* have used as continuum kinetic energy to study underdamped dynamics of strains in proper ferroelastic materials. The authors

obtain the next order term to the above continuum limit as shown below.

36. $$\gamma_{ss'}^{(1)}(\vec{k}) = \begin{pmatrix} \frac{1}{12} + \frac{k_x^4 + k_y^4}{8k_x^2k_y^2} & \frac{k_y^4 - k_x^4}{8k_x^2k_y^2} \\ \frac{k_y^4 - k_x^4}{8k_x^2k_y^2} & \frac{1}{12} + \frac{k_x^4 + k_y^4}{8k_x^2k_y^2} \end{pmatrix}$$

This term or equations 33 and 34 can be used to study the dynamics of proper ferroelastic materials on the atomic scale. The following long-wavelength limit of the atomic scale modes shows directly what they correspond to in the continuum theory.

37. $$e_1(\vec{i}) = \frac{1}{\sqrt{2}}[\nabla_x u_{\vec{i}}^x + \nabla_y u_{\vec{i}}^y]$$

38. $$e_2(\vec{i}) = \frac{1}{\sqrt{2}}[\nabla_x u_{\vec{i}}^y + \nabla_y u_{\vec{i}}^x]$$

39. $$e_3(\vec{i}) = \frac{1}{\sqrt{2}}[\nabla_x u_{\vec{i}}^x - \nabla_y u_{\vec{i}}^y]$$

40. $$r(\vec{i}) = \frac{1}{\sqrt{2}}[\nabla_x u_{\vec{i}}^y - \nabla_y u_{\vec{i}}^x]$$

41. $$s_x(\vec{i}) = \frac{1}{2}\nabla_x\nabla_y u_{\vec{i}}^x$$

42. $$s_y(\vec{i}) = \frac{1}{2}\nabla_x\nabla_y u_{\vec{i}}^y$$

43. $$t_x(\vec{i}) = 2u_{\vec{i}}^x$$

44. $$t_y(\vec{i}) = 2u_{\vec{i}}^y$$

In $k \to 0$ limit, the correspondence of these modes to the displacements u is

45. $$t_x, t_y \sim u$$
$$e_1, e_2, e_3, r \sim ku$$
$$s_x, s_y \sim k^2 u$$

The comparison shows that the approach is a natural extension of the continuum theory to the atomic scale and is suitable for multiscale description of lattice dynamics.

3. Quantum mechanical formalism

3.1 One-dimensional lattice with a monatomic basis

It is necessary to consider quantum mechanical aspects of lattice dynamics for phenomena such as low-temperature specific heat, electron–phonon interaction and polarons. In this section, the authors extend the symmetry-based atomic scale description of lattice dynamics to the quantum mechanical formalism. Commutation relations between the coordinate operators and their conjugate momentum operators lie at the core of quantum mechanics, which the authors establish here for the symmetry modes.

First, the authors consider the one-dimensional chain studied in section 2.1. The conjugate momenta for the two modes, $P_e(i)$ and $P_t(i)$, are

46. $$P_e(i) = \frac{\partial L}{\partial \dot{e}(i)} = \frac{M}{2}\dot{e}(i) = \frac{1}{2\sqrt{2}}(p_{i+1} - p_i)$$

47. $$P_t(i) = \frac{\partial L}{\partial \dot{t}(i)} = \frac{M}{2}\dot{t}(i) = \frac{1}{2\sqrt{2}}(p_{i+1} + p_i)$$

where p_i represents the momentum of the atom at site i. From known commutation relations between momentum and displacement operators, $\hat{p}_i$ and $\hat{u}_j$, the authors find the following commutation relations between the operators for modes and their conjugate momenta with the same site index i,

48. $$[P_a(i), b(i)] = \frac{\hbar}{2i}\delta_{ab}$$

where $a, b \in \{e, t\}$. The 1/2 factor is related to the number of atoms in each motif. Unlike displacement variables, the commutation relation between a mode at i and a conjugate momentum at $i+1$ or $i-1$ is not zero, since they share an atom, as shown below.

49. $$[P_t(i), t(i \pm 1)] = [P_e(i), t(i+1)] = [P_t(i), e(i-1)] = \frac{\hbar}{4i}$$

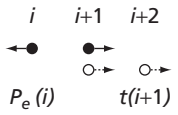

Figure 6. Graph to find commutation relation, $[P_e(i), t(i+1)]$.

50. $$[P_e(i), e(i\pm1)] = [P_t(i), e(i+1)] = [P_e(i), t(i-1)] = \frac{-\hbar}{4i}$$

The commutation relations between the momentum and the mode, defined at sites further than the nearest neighbors, vanish.

The above relations are also established graphically. For example, $[P_e(i),t(i+1)]$ is found from the drawing in Figure 6, where $P_e(i)$ and $t(i+1)$ are represented with arrows. The authors treat the arrows as unit vectors and find the sum of scalar products of unit vectors defined at the same sites, which after being multiplied by $\hbar/(2^2 i)$, lead to the commutation relation. From the graphical rule and the symmetry of the modes, the following commutations are obtained, where $a,b \in \{e,t\}$.

51. $$\left[P_a(i), b(j)\right] = \left[P_b(j), a(i)\right]$$

52. $$\left[P_e(i),t(j)\right] = -\left[P_t(i),e(j)\right]$$

The commutation relations in reciprocal space are calculated from the relations,

53. $$\left[P_a(k),b(k')\right] = \delta_{k',-k}\sum_j [P_a(i=0),b(j)]e^{ikj}$$

which are shown in Table 1. The results found here are applicable, for example, for the study of quantum mechanical dynamics of nonlinear excitations mentioned in section 2.1.

3.2 Two-dimensional square lattice with a monatomic basis

Quantum mechanical nature of lattice is also important for two- or three-dimensional lattices, for example, near the structural phase transitions or complex emergent materials with competing structural phases. In this subsection, the authors find quantum mechanical commutation relations for the symmetry modes and their conjugate momenta for the square lattice studied in section 2.2.

	$\frac{i}{\hbar}P_e(k)$	$\frac{i}{\hbar}P_t(k)$
e(–k)	$\frac{1}{2}(1-\cos k)$	$-\frac{i}{2}\sin k$
t(–k)	$\frac{i}{2}\sin k$	$\frac{1}{2}(1+\cos k)$

Table 1. Commutation relation, $[iP_a(k)/\hbar, b(-k)]$, between symmetry modes and their conjugate momenta for the one dimensional chain in reciprocal space.

Conjugate momenta for the atomic scale symmetry modes are as follows:

54.
$$P_{e_1}(\vec{i}) = \frac{M}{4}\dot{e}_1(\vec{i}) = \frac{1}{8\sqrt{2}}\left(-p_{\vec{i}}^x - p_{\vec{i}}^y + p_{\vec{i}+10}^x - p_{\vec{i}+10}^y - p_{\vec{i}+01}^x + p_{\vec{i}+01}^y + p_{\vec{i}+11}^x + p_{\vec{i}+11}^y\right)$$
$$P_{e_2}(\vec{i}) = \frac{M}{4}\dot{e}_2(\vec{i}) = \frac{1}{8\sqrt{2}}\left(-p_{\vec{i}}^x - p_{\vec{i}}^y - p_{\vec{i}+10}^x + p_{\vec{i}+10}^y + p_{\vec{i}+01}^x - p_{\vec{i}+01}^y + p_{\vec{i}+11}^x + p_{\vec{i}+11}^y\right)$$
$$P_{e_3}(\vec{i}) = \frac{M}{4}\dot{e}_3(\vec{i}) = \frac{1}{8\sqrt{2}}\left(-p_{\vec{i}}^x + p_{\vec{i}}^y + p_{\vec{i}+10}^x + p_{\vec{i}+10}^y - p_{\vec{i}+01}^x - p_{\vec{i}+01}^y + p_{\vec{i}+11}^x - p_{\vec{i}+11}^y\right)$$
$$P_r(\vec{i}) = \frac{M}{4}\dot{r}(\vec{i}) = \frac{1}{8\sqrt{2}}\left(p_{\vec{i}}^x - p_{\vec{i}}^y + p_{\vec{i}+10}^x + p_{\vec{i}+10}^y - p_{\vec{i}+01}^x - p_{\vec{i}+01}^y - p_{\vec{i}+11}^x + p_{\vec{i}+11}^y\right)$$
$$P_{s_x}(\vec{i}) = \frac{M}{4}\dot{s}_x(\vec{i}) = \frac{1}{8}\left(p_{\vec{i}}^x - p_{\vec{i}+10}^x - p_{\vec{i}+01}^x + p_{\vec{i}+11}^x\right)$$
$$P_{s_y}(\vec{i}) = \frac{M}{4}\dot{s}_y(\vec{i}) = \frac{1}{8}\left(p_{\vec{i}}^y - p_{\vec{i}+10}^y - p_{\vec{i}+01}^y + p_{\vec{i}+11}^y\right)$$
$$P_{t_x}(\vec{i}) = \frac{M}{4}\dot{t}_x(\vec{i}) = \frac{1}{8}\left(p_{\vec{i}}^x + p_{\vec{i}+10}^x + p_{\vec{i}+01}^x + p_{\vec{i}+11}^x\right)$$
$$P_{t_y}(\vec{i}) = \frac{M}{4}\dot{t}_y(\vec{i}) = \frac{1}{8}\left(p_{\vec{i}}^y + p_{\vec{i}+10}^y + p_{\vec{i}+01}^y + p_{\vec{i}+11}^y\right)$$

From the fundamental commutation relations for displacement operators and momentum operators,

55.
$$[p_{\vec{i}}^x, u_{\vec{j}}^x] = [p_{\vec{i}}^y, u_{\vec{j}}^y] = \frac{\hbar}{i}\delta_{\vec{i},\vec{j}}$$
$$[p_{\vec{i}}^x, u_{\vec{j}}^y] = [p_{\vec{i}}^y, u_{\vec{j}}^x] = 0$$

the commutation relations between modes and their conjugate momenta are calculated in a straight-forward way.

However, it is more convenient to use the graphical method, explained for the one-dimensional chain in the previous subsection. The above fundamental commutation relations for $\vec{i} = \vec{j}$ have the form of

56. $$\hat{x}\cdot\hat{x}=\hat{y}\cdot\hat{y}=1$$
$$\hat{x}\cdot\hat{y}=\hat{y}\cdot\hat{x}=0$$

except for the factor $\hbar/i$, where $\hat{x}$ and $\hat{y}$ represent unit vectors, not operators. Therefore, the commutation relation $[P_a(\vec{i}),b(\vec{j})]$, where a and b represent the eight atomic scale modes, is found from the drawings of a and b modes on the square lattice. The sum of the scalar products of the unit vectors at the sites shared by the two modes, multiplied by $\hbar/(4^2 i)$, gives the commutation of the two operators. (The multiplication factor after $\hbar/i$ is associated with the number of atoms in the motif for the lattice with a monatomic basis, that is four for the square lattice and two for the chain.) For example, $[P_{e1}(\vec{i}),e_2(\vec{i}+11)]$ is found from Figure 7, as follows:

57. $$[P_{e1}(\vec{i}),e_2(\vec{i}+11)]=\frac{\hbar}{4^2 i}(-1)$$

Presented graphical method is also useful to find the following symmetry-related properties of the commutation relations, where a and b represent any of the eight modes, and even and odd represent the modes with even symmetry under point reflection, namely, e_1, e_2, e_3, r, and the modes with odd symmetry, namely, s_x, s_y, t_x, t_y, respectively.

58. $$\begin{aligned}[P_a(\vec{i}),b(\vec{i})]&=\frac{1}{4}\frac{\hbar}{i}\delta_{ab}\\ [P_a(\vec{i}),b(\vec{j})]&=[P_b(\vec{j}),a(\vec{i})]\\ [P_{even}(\vec{i}),even'(\vec{j})]&=[P_{even'}(\vec{i}),even(\vec{j})]\\ [P_{even}(\vec{i}),odd(\vec{j})]&=-[P_{odd}(\vec{i}),even(\vec{j})]\\ [P_{odd}(\vec{i}),odd'(\vec{j})]&=[P_{odd'}(\vec{i}),odd(\vec{j})]\end{aligned}$$

The commutation relations in reciprocal space are found from the below relation, which are provided in Table 2.

59. $$[P_a(\vec{k}),b(\vec{k}')]=\delta_{\vec{k}',-\vec{k}}\sum_{\vec{j}}[P_a(\vec{i}=0),b(\vec{j})]e^{i\vec{k}\cdot\vec{j}}$$

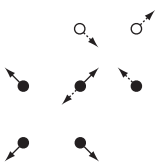

Figure 7. Graph to find commutation relation, $[P_{e1}(\vec{i}), e_2(\vec{i}+11)]$.

4. Example of the application of symmetry modes for lattice dynamics

As a simple demonstration for the application of symmetry modes, the analyze phonon modes in terms of atomic scale symmetry modes for the square lattice with a harmonic potential shown below.

60. $$\begin{aligned}V_{sq}=\sum_{\vec{i}}&\frac{1}{2}A_1e_1(\vec{i})^2+\frac{1}{2}A_2e_2(\vec{i})^2+\frac{1}{2}A_3e_3(\vec{i})^2\\&+\frac{1}{2}B[s_x(\vec{i})^2+s_y(\vec{i})^2]\end{aligned}$$

The phonon dispersion relation for this potential energy was presented previously.[12] Furthermore, the phonon mode at $\vec{k}=(\pi,\pi)$, both in the upper and the lower branch, was shown entirely composed of short-wave length modes, s_x and s_y, due to the constraints. In general, at other $\vec{k}$ points, the contribution of different symmetry modes to the phonon mode depends not only on the constraint equations but also on the values of the elastic moduli in the energy expression. In this section, the authors present the study on how different symmetry modes generally contribute to phonon modes for the entire first Brillouin zone for the potential V_{sq} shown above.

The equation of motion using conventional displacement-based approach leads the expression for the normal mode at $\vec{k}$, $[u_x^{\pm}(\vec{k}),u_y^{\pm}(\vec{k})]$ except for an overall factor, where ± represents the upper and lower branches. By using the $\vec{k}$-space relation between symmetry modes and displacements, which is obtained from equations 11–20, the authors obtained the expression of $[e_1^{\pm}(\vec{k}),e_2^{\pm}(\vec{k}),e_3^{\pm}(\vec{k}),r^{\pm}(\vec{k}),s_x^{\pm}(\vec{k}),s_y^{\pm}(\vec{k}),t_x^{\pm}(\vec{k}),t_y^{\pm}(\vec{k})]$ for the phonon modes at $\vec{k}$, where ± again represents the upper and the lower branches. (This can be also performed without explicit use of displacement variables, as suggested by equation 31 and performed for the 1D chain.) The results are shown in Table 3, where $\beta_1=1-\cos k_x\cos k_y$, $\beta_2=-\sin k_x\sin k_y$, $\beta_3=\cos k_x-\cos k_y$, $\beta_4=(1-\cos k_x)(1-\cos k_y)$, $\beta_5=(1+\cos k_x)(1+\cos k_y)$, and $a=(A_1-A_2+A_3)/(A_1+A_2-A_3)$. In this result, the overall factor of the normal mode is determined by the normalization condition

61. $$|u_x^{\pm}(\vec{k})|^2+|u_y^{\pm}(\vec{k})|^2=4$$

that is,

62. $$\begin{aligned}&|e_1^{\pm}(\vec{k})|^2+|e_2^{\pm}(\vec{k})|^2+|e_3^{\pm}(\vec{k})|^2+|r^{\pm}(\vec{k})|^2+|s_x^{\pm}(\vec{k})|^2\\&+|s_y^{\pm}(\vec{k})|^2+|t_x^{\pm}(\vec{k})|^2+|t_y^{\pm}(\vec{k})|^2=1\end{aligned}$$

To be specific, the authors show these expressions for a special case of $a=1$, which corresponds to $A_2=A_3$, in the last column of Table 3 and plot them within the first Brillouin zone of the square lattice in Figure 8. The results show the anisotropic contributions of different symmetry modes to the upper- and the lower-branch phonon modes

	$\frac{i}{\hbar}P_{e1,k}$	$\frac{i}{\hbar}P_{e2,k}$	$\frac{i}{\hbar}P_{e3,k}$	$\frac{i}{\hbar}P_{\gamma,k}$	$\frac{i}{\hbar}P_{sx,k}$	$\frac{i}{\hbar}P_{sy,k}$	$\frac{i}{\hbar}P_{tx,k}$	$\frac{i}{\hbar}P_{ty,k}$
$e_{1,-k}$	$\frac{1-C_xC_y}{4}$	$\frac{S_xS_y}{4}$	$\frac{-C_x+C_y}{4}$	0	$\frac{i(1-C_x)S_y}{4\sqrt{2}}$	$\frac{i(1-C_y)S_x}{4\sqrt{2}}$	$\frac{i(1+C_y)S_x}{-4\sqrt{2}}$	$\frac{i(1+C_x)S_y}{-4\sqrt{2}}$
$e_{2,-k}$	$\frac{S_xS_y}{4}$	$\frac{1-C_xC_y}{4}$	0	$\frac{-C_x+C_y}{4}$	$\frac{i(1-C_y)S_x}{4\sqrt{2}}$	$\frac{i(1-C_x)S_y}{4\sqrt{2}}$	$\frac{i(1+C_x)S_y}{-4\sqrt{2}}$	$\frac{i(1+C_y)S_x}{-4\sqrt{2}}$
$e_{3,-k}$	$\frac{-C_x+C_y}{4}$	0	$\frac{1-C_xC_y}{4}$	$\frac{-S_xS_y}{4}$	$\frac{i(1-C_x)S_y}{4\sqrt{2}}$	$\frac{i(1-C_y)S_x}{-4\sqrt{2}}$	$\frac{i(1+C_y)S_x}{-4\sqrt{2}}$	$\frac{i(1+C_x)S_y}{4\sqrt{2}}$
r_{-k}	0	$\frac{-C_x+C_y}{4}$	$\frac{-S_xS_y}{4}$	$\frac{1-C_xC_y}{4}$	$\frac{i(1-C_y)S_x}{-4\sqrt{2}}$	$\frac{i(1-C_x)S_y}{4\sqrt{2}}$	$\frac{i(1+C_x)S_y}{4\sqrt{2}}$	$\frac{i(1+C_y)S_x}{-4\sqrt{2}}$
$s_{x,-k}$	$\frac{i(1-C_x)S_y}{-4\sqrt{2}}$	$\frac{i(1-C_y)S_x}{-4\sqrt{2}}$	$\frac{i(1-C_x)S_y}{-4\sqrt{2}}$	$\frac{i(1-C_y)S_x}{4\sqrt{2}}$	$\frac{(1-C_x)(1-C_y)}{4}$	0	$\frac{-S_xS_y}{4}$	0
$s_{y,-k}$	$\frac{i(1-C_y)S_x}{-4\sqrt{2}}$	$\frac{i(1-C_x)S_y}{-4\sqrt{2}}$	$\frac{i(1-C_y)S_x}{4\sqrt{2}}$	$\frac{i(1-C_x)S_y}{-4\sqrt{2}}$	0	$\frac{(1-C_x)(1-C_y)}{4}$	0	$\frac{-S_xS_y}{4}$
$t_{x,-k}$	$\frac{i(1+C_y)S_x}{4\sqrt{2}}$	$\frac{i(1+C_x)S_y}{4\sqrt{2}}$	$\frac{i(1+C_y)S_x}{4\sqrt{2}}$	$\frac{i(1+C_x)S_y}{-4\sqrt{2}}$	$\frac{-S_xS_y}{4}$	0	$\frac{(1+C_x)(1+C_y)}{4}$	0
$t_{y,-k}$	$\frac{i(1+C_x)S_y}{4\sqrt{2}}$	$\frac{i(1+C_y)S_x}{4\sqrt{2}}$	$\frac{i(1+C_x)S_y}{-4\sqrt{2}}$	$\frac{i(1+C_y)S_x}{4\sqrt{2}}$	0	$\frac{-S_xS_y}{4}$	0	$\frac{(1+C_x)(1+C_y)}{4}$

Table 2. Commutation relation, $[iP_a(\vec{k})/\hbar, b(-\vec{k})]$, between symmetry modes and their conjugate momenta for the two dimensional square lattice in reciprocal space. C_x, C_y, S_x and S_y represent cos k_x, cos k_y, sin k_x, and sink_y, respectively.

within the first Brillouin zone. Some of the features are discussed in the figure caption.

5. Discussion

In this section, the authors briefly discuss how the approach can be used for complex materials in which nonlinearity in elastic energy is important. Because this approach uses modes based on the symmetry of lattice, it can be useful for atomic scale description of dynamics in solid–solid phase transitions.

For example, the following second-order-like double well potential energy introduced previously[12] represents a system with degenerate ground states of rectangular lattices with different orientations,

$$63.\quad V_{\text{rec}} = \sum_{\vec{i}} \frac{1}{2}A_1e_1(\vec{i})^2 + \frac{1}{2}A_2e_2(\vec{i})^2 - \frac{1}{2}A_3{'}e_3(\vec{i})^2 + \frac{1}{4}F_3e_3(\vec{i})^4 + \frac{1}{2}B[s_x(\vec{i})^2 + s_y(\vec{i})^2]$$

Therefore, the following Lagrangian can be used to study atomic scale dynamics related to the square to rectangular lattice phase transition,

$$64.\quad L_{\text{rec}} = T_{\text{sq}} - V_{\text{rec}}$$

As another example, the following first-order-like potential energy, introduced previously related to the phase coexistence in perovskite manganites,[8] represents the competition between high-symmetry phase with undistorted square lattice and degenerate low-symmetry phases with rectangular and staggered lattice distortions for certain ranges of parameter values,

$$65.\quad V_{\text{multi}} = V_{\text{short}} + V_{\text{long}} + V_{\text{coupling}}$$

$$66.\quad V_{\text{short}} = \sum_{\vec{i}} \frac{B}{2}[s_x(\vec{i})^2 + s_y(\vec{i})^2] + \frac{G_1}{4}[s_x(\vec{i})^4 + s_y(\vec{i})^4] + \frac{G_2}{2}s_x(\vec{i})^2s_y(\vec{i})^2 + \frac{H_1}{6}[s_x(\vec{i})^6 + s_y(\vec{i})^6] + \frac{H_2}{6}s_x(\vec{i})^2s_y(\vec{i})^2[s_x(\vec{i})^2 + s_y(\vec{i})^2]$$

Mode	General expression (upper/lower branch)	Special case: a = 1	
		Upper branch	Lower branch
$\lvert e_1(\vec{k})\rvert^2$	$\frac{1}{8}\left(\beta_1 \pm \frac{\beta_2^2 + a\beta_3^2}{\sqrt{\beta_2^2 + a^2\beta_3^2}}\right)$	$\frac{\beta_1}{4}$	0
$\lvert e_2(\vec{k})\rvert^2$	$\frac{1}{8}\left(\beta_1 \pm \frac{\beta_2^2 - a\beta_3^2}{\sqrt{\beta_2^2 + a^2\beta_3^2}}\right)$	$\frac{\beta_2^2}{4\beta_1}$	$\frac{\beta_3^2}{4\beta_1}$
$\lvert e_3(\vec{k})\rvert^2$	$\frac{1}{8}\left(\beta_1 \mp \frac{\beta_2^2 - a\beta_3^2}{\sqrt{\beta_2^2 + a^2\beta_3^2}}\right)$	$\frac{\beta_3^2}{4\beta_1}$	$\frac{\beta_2^2}{4\beta_1}$
$\lvert r(\vec{k})\rvert^2$	$\frac{1}{8}\left(\beta_1 \mp \frac{\beta_2^2 + a\beta_3^2}{\sqrt{\beta_2^2 + a^2\beta_3^2}}\right)$	0	$\frac{\beta_1}{4}$
$\lvert s_x(\vec{k})\rvert^2$	$\frac{\beta_4}{8}\left(1 \mp \frac{a\beta_3}{\sqrt{\beta_2^2 + a^2\beta_3^2}}\right)$	$\frac{\beta_4}{8\beta_1}(\beta_1 - \beta_3)$	$\frac{\beta_4}{8\beta_1}(\beta_1 + \beta_3)$
$\lvert s_y(\vec{k})\rvert^2$	$\frac{\beta_4}{8}\left(1 \pm \frac{a\beta_3}{\sqrt{\beta_2^2 + a^2\beta_3^2}}\right)$	$\frac{\beta_4}{8\beta_1}(\beta_1 + \beta_3)$	$\frac{\beta_4}{8\beta_1}(\beta_1 - \beta_3)$
$\lvert t_x(\vec{k})\rvert^2$	$\frac{\beta_5}{8}\left(1 \mp \frac{a\beta_3}{\sqrt{\beta_2^2 + a^2\beta_3^2}}\right)$	$\frac{\beta_5}{8\beta_1}(\beta_1 - \beta_3)$	$\frac{\beta_5}{8\beta_1}(\beta_1 + \beta_3)$
$\lvert t_y(\vec{k})\rvert^2$	$\frac{\beta_5}{8}\left(1 \pm \frac{a\beta_3}{\sqrt{\beta_2^2 + a^2\beta_3^2}}\right)$	$\frac{\beta_5}{8\beta_1}(\beta_1 + \beta_3)$	$\frac{\beta_5}{8\beta_1}(\beta_1 - \beta_3)$
$\lvert s_+(\vec{k})\rvert^2$	$\frac{\beta_4}{8}\left(1 \mp \frac{\beta_2}{\sqrt{\beta_2^2 + a^2\beta_3^2}}\right)$	$\frac{\beta_4}{8\beta_1}(\beta_1 - \beta_2)$	$\frac{\beta_4}{8\beta_1}(\beta_1 + \beta_2)$
$\lvert s_-(\vec{k})\rvert^2$	$\frac{\beta_4}{8}\left(1 \pm \frac{\beta_2}{\sqrt{\beta_2^2 + a^2\beta_3^2}}\right)$	$\frac{\beta_4}{8\beta_1}(\beta_1 + \beta_2)$	$\frac{\beta_4}{8\beta_1}(\beta_1 - \beta_2)$
$\lvert t_+(\vec{k})\rvert^2$	$\frac{\beta_5}{8}\left(1 \mp \frac{\beta_2}{\sqrt{\beta_2^2 + a^2\beta_3^2}}\right)$	$\frac{\beta_5}{8\beta_1}(\beta_1 - \beta_2)$	$\frac{\beta_5}{8\beta_1}(\beta_1 + \beta_2)$
$\lvert t_-(\vec{k})\rvert^2$	$\frac{\beta_5}{8}\left(1 \pm \frac{\beta_2}{\sqrt{\beta_2^2 + a^2\beta_3^2}}\right)$	$\frac{\beta_5}{8\beta_1}(\beta_1 + \beta_2)$	$\frac{\beta_5}{8\beta_1}(\beta_1 - \beta_2)$

For ± and ∓, the upper sign corresponds to the upper branch, and the lower sign indicates the lower branch. $\beta_1 = 1-\cos k_x \cos k_y$, $\beta_2 = -\sin k_x \sin k_y$, $\beta_3 = \cos k_x - \cos k_y$, $\beta_4 = (1-\cos k_x)(1-\cos k_y)$, $\beta_5 = (1+\cos k_x)(1+\cos k_y)$, and $a = (A_1 - A_2 + A_3)/(A_1 + A_2 - A_3)$. Symmetry exists between upper and lower branches. For example, $|e_1(\vec{k})|^2$ in upper branch has identical expression as $|r(\vec{k})|^2$ in the lower branch. In fact, all eight modes can be related in similar ways. Special case of $a = 1$ corresponds to the case of $A_2 = A_3$.

Table 3. Normalized symmetry-mode squared amplitude for phonons within the first Brillouin zone of the square lattice.

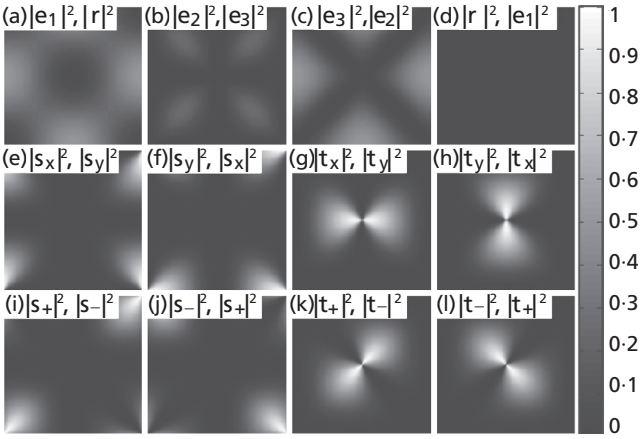

Figure 8. Normalized symmetry-mode squared amplitude for phonons within the first Brillouin zone of the square lattice for $A_2 = A_3$, that is, a = 1. The center of each square corresponds $\vec{k} = (0,0)$ to $\vec{k} = (\pm\pi, \pm\pi)$ and the four corners . The first and the second label for each panel indicate the mode for upper branch and lower branch, respectively. Therefore, for the upper branch, the twelve panels correspond to (a) $|e_1|^2$, (b) $|e_2|^2$, (c) $|e_3|^2$, (d) $|r|^2$, (e) $|s_x|^2$, (f) $|s_y|^2$, (g) $|t_x|^2$, (h) $|t_y|^2$, (i) $|s_+|^2$, (j) $|s_-|^2$, (k) $|t_+|^2$ and (l) $|t_-|^2$. For the lower branch, they correspond to (a) $|r|^2$, (b) $|e_3|^2$, (c) $|e_2|^2$, (d) $|e_1|^2$, (e) $|s_y|^2$, (f) $|s_x|^2$, (g) $|t_y|^2$, (h) $|t_x|^2$, (i) $|s_-|^2$, (j) $|s_+|^2$, (k) $|t_-|^2$ and (l) $|t_+|^2$. Panel (d) shows that the upper and lower branches of phonon modes remain locally rotationless and area preserving, respectively, in this particular case of $A_2 = A_3$. This feature can be understood easily in the long-wavelength limit from the fact that the sound velocity is isotropic for $A_2 = A_3$, and therefore the lattice supports longitudinal (rotationless) and transverse (area preserving) phonon modes. Such isotropic sound velocity for crystals can be useful for device applications.

$$67. \quad V_{\text{long}} = \sum_{\vec{i}} \frac{1}{2} A_1 e_1(\vec{i})^2 + \frac{1}{2} A_2 e_2(\vec{i})^2 + \frac{1}{2} A_3 e_3(\vec{i})^2$$

$$68. \quad V_{\text{coupling}} = \sum_{\vec{i}} C_3 [s_x(\vec{i})^2 - s_y(\vec{i})^2] e_3(\vec{i})$$

How the competition between the ground state and metastable local energy minimum states can influence the atomic scale dynamics of solid–solid phase transitions can be studied from the following Lagrangian,

$$69. \quad L_{\text{multi}} = T_{\text{sq}} - V_{\text{multi}}$$

So far, the dynamics with the above potential energies has been studied with the steepest decent or the Euler method to find stable domain configurations.[8,12] With the proper kinetic energy expression in symmetry modes presented in this article, more realistic dynamics related to the solid–solid phase transitions in complex materials can be simulated for both second-order-like and first-order-like potential energy expressions shown above. The phenomenological approach complements existing molecular dynamic approaches, which apply pair potentials, such as the Lennard-Jones potential.

6. Conclusion

In this article, the authors have presented mode-based atomic scale description of lattice dynamics. It is found that not only the potential energy but also the kinetic energy is described in terms of the atomic scale modes, for which the inclusion of the rigid modes is essential. This approach has been demonstrated for the one-dimensional chain and the two-dimensional square lattice with a monatomic basis. The comparison with a continuum model has shown that the approach is suitable for multiscale description of lattice dynamics. The approach has been extended to quantum mechanics, and the commutation relations have been obtained. As an example, the phonon modes are analyzed in terms of symmetry modes. The authors also discuss how the approach can be used to study atomic scale dynamics associated with solid–solid structural phase transitions in complex emergent materials, in which competition between phases with different lattice structures is important, and therefore, the nonlinearity of lattice energy needs to be considered properly.

REFERENCES

1. Rini, M.; Tobey, R.; Dean, N.; Itatani, J.; Tomioka, Y.; Tokura, Y.; Schoenlein, R. W.; Cavalleri, A. Control of the electronic phase of a manganite by mode-selective vibrational excitation. *Nature* **2007**, *449*, 72–74.
2. Salamon, M. B.; Jaime, M. The physics of manganites: structure and transport. *Reviews of Modern Physics* **2001**, *73*, 583–628.
3. Millis, A. J. Lattice effects in magnetoresistive manganese perovskites. *Nature* **1998**, *392*, 147–150.
4. Jin, S.; Tiefel, T. H.; McCormack, M.; Fastnacht, R. A.; Ramesh, R.; Chen, L. H. Thousandfold change in resistivity in magnetoresistive La-Ca-Mn-O films. *Science* **1994**, *264*, 413–415.
5. Tranquada, J. M.; Sternlieb, B. J.; Axe, J. D.; Nakamura, Y.; Uchida, S. Evidence for stripe correlations of spins and holes in copper oxide superconductors. *Nature* **1995**, *375*, 561–563.
6. Kivelson, S. A.; Bindloss, I. P.; Fradkin, E.; Oganesyan, V.; Tranquada, J. M.; Kapitulnik, A.; Howald, C. How to detect fluctuating stripes in the high-temperature superconductors. *Reviews of Modern Physics* **2003**, *75*, 1201–1241.
7. Kiryukhin, V. Nanoscale structural correlations in magnetoresistive manganites. *New Journal of Physics* **2004**, *6*, 155.
8. Ahn, K. H.; Lookman, T.; Bishop, A. R. Strain-induced metal-insulator phase coexistence in perovskite manganites. *Nature* **2004**, *428*, 401–404.

9. Gaffney, K. J.; Chapman, H. N. Imaging atomic structure and dynamics with ultrafast x-ray scattering. *Science* **2005**, *316*, 1444–1448.
10. Shenoy, S. R.; Lookman, T.; Saxena, A.; Bishop, A. R. Martensitic textures: multiscale consequences of elastic compatibility. *Physical Review B: Condensed Matter and Materials Physics* **1999**, *60*, R12537–R12541.
11. Lookman, T.; Shenoy, S. R.; Rasmussen, K. Ø.; Saxena, A.; Bishop, A. R. Ferroelastic dynamics and strain compatibility. *Physical Review B: Condensed Matter and Materials Physics* **2003**, *67*, 024114.
12. Ahn, K. H.; Lookman, T.; Saxena, A.; Bishop, A. R. Atomic scale lattice distortions and domain wall profiles. *Physical Review B: Condensed Matter and Materials Physics* **2003**, *68*, 092101.
13. Ahn, K. H.; Lookman, T.; Saxena, A.; Bishop, A. R. Electronic properties of structural twin and antiphase boundaries in materials with strong electron-lattice couplings. *Physical Review B: Condensed Matter and Materials Physics* **2005**, *71*, 212102.
14. Zhu, J.-X.; Ahn, K. H.; Nussinov, Z.; Lookman, T.; Balatsky, A. V.; Bishop, A. R. Elasticity-driven nanoscale electronic structure in superconductors. *Physical Review Letters* **2003**, *91*, 057004.
15. Doh, H.; Kim, Y. B.; Ahn, K. H. Nematic domains and resistivity in an itinerant metamagnet coupled to phonons. *Physical Review Letters* **2007**, *98*, 126407.
16. Kittel, C. *Introduction to Solid State Physics*, 8th edn. Singapore: John Wiley and Sons, Inc., 2004.
17. Chen, D.; Aubry, S.; Tsironis, G. P. Breather mobility in discrete φ4 nonlinear lattices. *Physical Review Letters* **1996**, *77*, 4776–4779.
18. Kosevich, Y. A.; Manevitch, L. I.; Savin, A. V. Wandering breathers and self-trapping in weakly coupled nonlinear chains: classical counterpart of macroscopic tunneling quantum dynamics. *Physical Review E* **2008**, *77*, 046603.
19. Atkins, P. W.; Friedman, R. S. *Molecular Quantum Mechanics*, 5th edn. New York: Oxford University Press, 2010.